Received: 22 February 2019
DOI: 10.1002/mop.32020

WILEY

RESEARCH ARTICLE

A novel application of artificial neural network for recognition of target behind the wall

Akhilendra P. Singh[1] | **Smrity Dwivedi**[1] | **Pradip K. Jain**[1,2]

[1]Department of Electronics Engineering, Indian Institute of Technology (BHU), Varanasi, India

[2]Department of Electronics and Communication Engineering, National Institute of Technology Patna, Patna, India

Correspondence
Akhilendra P. Singh, Department of Electronics Engineering, Indian Institute of Technology (BHU), Varanasi, India.
Email: apsingh.rs.ece14@itbhu.ac.in

Abstract

In this article, a methodology for recognition of an object behind a wall has been proposed. So far research is mainly focused on target detection and localization issue. Very limited work has been reported so far for complete identification (ie, shape and size) of the target. Therefore in this article, a novel Artificial Neural Network based technique is proposed for identification of the targets behind the wall with the through the wall imaging system. For this purpose, an active microwave imaging radar system operating at frequency 3.5-5.5 GHz has been ingeniously designed. An extensive number of experiments were performed while keeping targets made of metal and wood in different shapes and sizes. For identification of the target, an artificial neural network based image reconstruction model has been proposed. From experimental results, it was found that once training of proposed neural network with sample teaching images has been done, it could automatically rectify distortions and reconstruct nearly actual shape and size of the target for test targets. The obtained results are quite satisfactory.

KEYWORDS

artificial neural network, mean, microwave imaging, shape and size estimation, SD, through wall radar imaging

1 | INTRODUCTION

Through-the-wall radar imaging (TWRI) system is an evolving technology, which enables the user to detect objects behind a wall from a certain standoff position. These systems use electromagnetic (EM) waves, which can penetrate the wall to sense objects inside an enclosed building. TWRI systems have various application civilian and military applications surveillance, indoor security, search and rescue mission of objects inside a building and a lot more. For military applications, these systems can be used to detect concealed objects such as terrorists hiding inside a building. Further, in rescue applications, TWRI system can also be used to detect survivors under rubble after a natural disaster such as an earthquake. Having various civilian and military applications, TWRI system faces various challenges which include target defocusing, target detection, and identification behind a wall from the images generated from TWRI system in presence of clutter and unwanted wall signal attenuation. There are several imaging algorithm images existing using various methodology as proposed by various authors[1-4] based on the prior knowledge of wall parameters (thickness and dielectric constant) but in a real scenario, the wrong estimation of these parameters could displace target from its actual position when the scene is being imaged. This problem is known as target defocusing. Many works has been done to address the target defocussing problem caused by a wall.[5-8] Another challenge, which exists is to detect the target from images generated by TWRI systems. The TWRI images of stationary target behind a wall are subject to strong clutter, which obscure the target image. This clutter is due to reflection from wall, environment, and multipath. Thus, there is a need to mitigate the clutter, which enhances the target in such a way that information of the presence of targets and their position becomes apparent. The foremost approach to mitigate clutter from strong wall reflection is based on background subtraction. This approach requires prior knowledge of the background scene. This approach gives good results but is not feasible in a real scenario because prior knowledge of the background scene cannot be obtained in a real scenario. As a result, in order to mitigate strong reflection from the wall without relying on prior knowledge of the background scene, some other approaches have been proposed such as statistical methods,[9-13] spatial filtering,[14] image fusion,[15,16] and so forth. The common aim of various detection methods is to generate a binary image from TWRI image depicting the position of the target.

Until now, most of the investigation has been done on the target detection[9-16] and classification[17,18] issues, while the other issues have not been explored well such as target identification. Therefore, an open challenge in TWRI applications would be recognition of the detected targets. Previously reported work on target recognition includes, use of inverse boundary scattering transform (IBST) on B-scan[19] and feature based artificial neural network on segmented objects from 2D C-scan image.[20] In contrast to algorithm proposed in,[20] a more promising technique for complete target identification could be the direct reconstruction of actual shape and size of target. For complete identification (ie, shape and size) of targets very limited work has been reported so far. Therefore, to recognize and visualize the actual shape and size of target behind a wall, a novel methodology using ANN has been proposed in this article. The present ANN model can reconstruct the actual target shape nullifying any rotation or size variations for the considered regular shapes. Thus, it would enable us to improve the quality of through-the-wall images.

In order to attain the above said objective an active microwave radar imaging system has been assembled for through the wall images formation. After that, these images for a number of targets have been used to train and develop the respective neural network model for target recognition, and later on, their capability was judged using an independent set of validation data, which has never been used for training. The article is organized as follows; section 2 describes measurement set up for through the wall imaging system. Section 3 describes the methodology for target identification. Validation of result is shown in section 4 and section 5 presents conclusions.

2 | MEASURMENT SET-UP FOR THROUGH THE WALL RADAR IMAGING SYSTEM

2.1 | Experimental design

The measurement setup for TWRI system[3] using SFCW radar is shown in Figure 1. SFCW radar has been assembled using Anritsu VNA (MS2037C), coaxial cable working and C-band horn antenna in the department of electronics engineering, Indian Institute of Technology (BHU), Varanasi, India. VNA is used for generation and demodulation of SFCW signals in frequency range of 3.5-5.5 GHz. C-band Horn antenna was used for transmitting and receiving the signal. It is placed on a 2D field scanner, which can move in horizontal direction and vertical direction. Table 1 shows typical value of designed SFCW radar parameters for imaging.

The radar is kept at 220 cm from the wall. The target is placed at 125 cm on another side of the wall. Four different shapes and sizes of wooden and metallic targets are considered. The target is placed on a wooden stand covered by absorbing sheet to minimize any reflection from the stand. The detail list of the target used for the purpose of target recognition is given in Table A1.

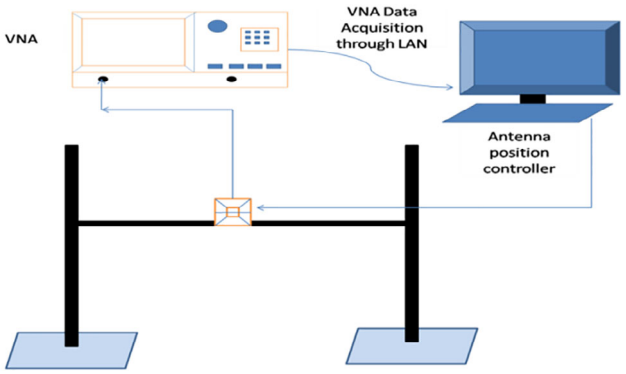

FIGURE 1 Measurement setup for through-the-wall radar imaging system[2] [Color figure can be viewed at wileyonlinelibrary.com]

TABLE 1 Typical values of SFCW radar parameters

Radar parameters	Value
Frequency range	3.5-5.5 GHz
Bandwidth	2GHz
Number of frequency points	201
Power transmitted	−3dbm
Range resolution	7.5 cm
Antenna type	Horn
Beam width	20°
Gain	18 dB

2.2 | Data acquisition

We have chosen a frequency range of 3.5-5.5 GHz for imaging. This frequency range has lower penetration loss through the wall. The range resolution depend upon bandwidth of system. Thus range resolution along downrange of SFCW radar for 2GHz bandwidth in free space will be 7.5 cm using Equation (1) as proposed by.[12]

$$\Delta Z = \frac{c}{2*BW} = 7.5cm \quad (1)$$

For capturing entire information of the scene behind walls, the target is scanned in the horizontal and vertical direction. The data have been collected using C-scan techniques for a stationary target kept behind a wall.

For this purpose, S-parameter S11 was collected from port 1 of VNA at 21 horizontal and 21 vertical scan points to completely cover the target. The inter-element spacing between each scan point is 5 cm. The number of frequency points decided the maximum unambiguous range, which can be calculated using Equation (2).[12]

$$z_{unambiguous} = \frac{c}{2X\Delta f} \quad (2)$$

where, Δf is frequency step size. However, based on target position in the downrange, maximum range has been limited to 5 m.

For development and validation of target recognition model, C-scan data have been collected for the metallic and wooden target of different shapes and size in a different orientation as given in Table 4. Thus, a total of 18 samples are captured by the TWRI system and the remaining 72 samples are generated virtually by morphological technique. Among the 90 samples, we have selected 90% of samples for the development of a methodology for recognition of target and the remaining 10% for validation of proposed methodology.

3 | THROUGH SIGNAL PROCESSING ALGORITHM FOR SHAPE AND SIZE ESTIMATION

Various signal processing steps are applied to data collected from the experiment in order to classify and estimate the shape and size of the target. Flowchart of different steps applied is shown in Figure 2 and a detail of each step is discussed below:

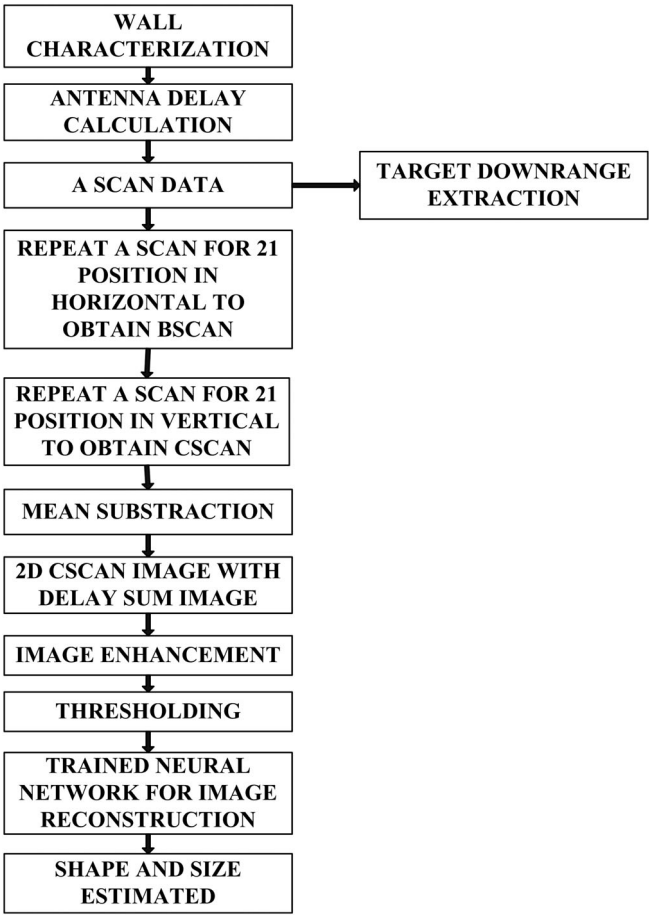

FIGURE 2 Flowchart of signal processing steps

3.1 | Preprocessing steps

For forming the image of the scene, three steps are very important. First to know the characteristics of the wall such as dielectric constant, this effect on the quality of image, antenna delay, and estimation of the downrange position of the target.

3.1.1 | Step 1. Wall characterization

An Estimate of wall dielectric has been done in a similar manner as proposed by Muqaible.[21] The average dielectric value of the wall was found to be 6.4.

3.1.2 | Step 2. Antenna delay calculation

In order to identify the delay due to the antenna system, a separate experiment is carried out in the same manner as proposed by.[12] A metallic plate is kept at known reference distance ($R_{reference}$) 2.20 m from radar. A-scan signal is obtained from the radar. After receiving the A-scan signal in the frequency domain, it is converted to equivalent range/distance domain, which is called a range profile using Equation (3) as proposed by[12]

$$s(z) = \sum_{m=1}^{201} S(f_k)\exp(j2\pi f_k(2z/c)) \quad (3)$$

The range profile plot as per Equation (3) is shown in Figure 3. The range profile shows the location of the metallic plate in front of the antenna in downrange. From the range profile, actual distance (R_{actual}) of the target from radar was found to be 3.111 m. Thus, antenna delay has been calculated using Equation (4) as proposed as

$$t_{delay} = \frac{R_{actual} - R_{reference}}{c} \quad (4)$$

3.1.3 | Step 3. Target downrange position estimation

A-scan signal obtained from radar kept at a specific position of 220 cm from the wall using measurement set up is processed to determine the accurate position of target behind a wall. The target is kept at 1.25 m on the side of the wall. Since, the A-scan signal obtained takes additional time in

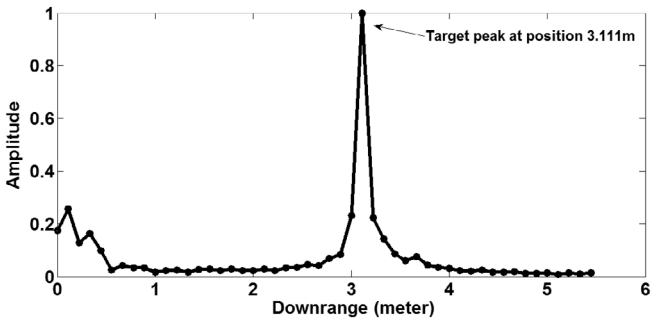

FIGURE 3 Range profile plot for equation 3

traveling from radar to target due to the delay of antenna system, and due to the different velocity of wave while propagating through the wall. Thus to determine the exact distance of the target, delay due to antenna and wall propagation is subtracted from target distance. The corrected range profile plot after correcting delays will be.[12]

$$s(\mathrm{z}) = \sum_{m=1}^{201} S(f_k)\exp\left(\begin{matrix} j2\pi f_k(2z/c + \\ R_{delay} + 2\mathrm{d}_{wall}\left(\sqrt{\varepsilon_{wall}} - 1\right)/\mathrm{c}) \end{matrix}\right) \quad (5)$$

Range profile plot using Equation (5) is shown in Figure 4. In range profile plot shown, the first two peaks are due to reflection from the front and rear side of the wall. The third peak shows the presence of a target. Thus, target downrange distance found to be 3.2 cm by observing the range profile.

3.2 | Post processing steps

3.2.1 | Step 4. Average subtraction

The received signal contains a reflected target as wells undesired signals. These undesired signals are present due to reflection from antenna mismatch, and background noise. To remove these undesired signals, average subtraction method is applied as proposed by.[12] For this purpose, the mean vector of each B-scan is calculated and further subtracted from its each individual A-scan[12]

$$B_{ij} = A_{ij} - \left(\frac{1}{21}\sum_{j=1}^{21} A_{ij}\right) \quad (6)$$

where, i = 1,2 … .21(number of B-scans), j = 1,2,…….21 (number of A-scans).

3.2.2 | Step 5. 2D C-scan image formation

The acquired C-scan data have been further processed for the formation of through the wall images using delay and sum beamforming. In delay and sum beamforming method, the virtual imaging plane is created, whose dimension is 50×50.

Figure 5 shows the geometry of through-the-wall imaging. The value of each pixel is estimated using the delay-and-sum wideband beamforming technique, which involves applying delays to the outputs of the C-scan data to synchronize the signal arrived all scan points and then summing the delayed signals using Equation (7) as proposed by.[2]

$$I\left(x_p\right) = \sum_{x=1}^{M}\sum_{y=1}^{N}\sum_{i=1}^{201} S(x,y)\exp\left\{j\omega_i\left(\tau_i - \tau_{antennadelay}\right)\right\} \quad (7)$$

S(x, y) is the radar signal at the mth frequency received by the antenna at position x, y, is the propagation delay encountered by the signal as it travels from scan point at position x, y to pixel positioned at, and back to same transceiver position. The delay is given by Equation (8) as proposed by.[2]

$$\tau_p = \frac{2l_{airtowall}}{c} + \frac{2l_{wall}}{v} + \frac{2l_{walltoair}}{c} \quad (8)$$

Here c is velocity of signal propagation in air and v is velocity of signal propagation through the wall. The variable $l_{airtowall}$, l_{wall}, $l_{walltoair}$ represents the distance traveled by the signal before, through and beyond the wall from mth antenna at position x, y to the target at position x_p. The details calculation of delay is discussed in.[2]

If the image pixel and antenna are at the same height then propagation delay and complex pixel value has been calculated in similar fashion using Equation (8) and if image pixel and antenna are at different height then a rotation transform has been applied to x, y, z coordinate system such that angle of incidence is preserved so that in new coordinate system image pixel and antenna appears to be at the same height. This transformation is given by[2] using Equations (9)-(12)

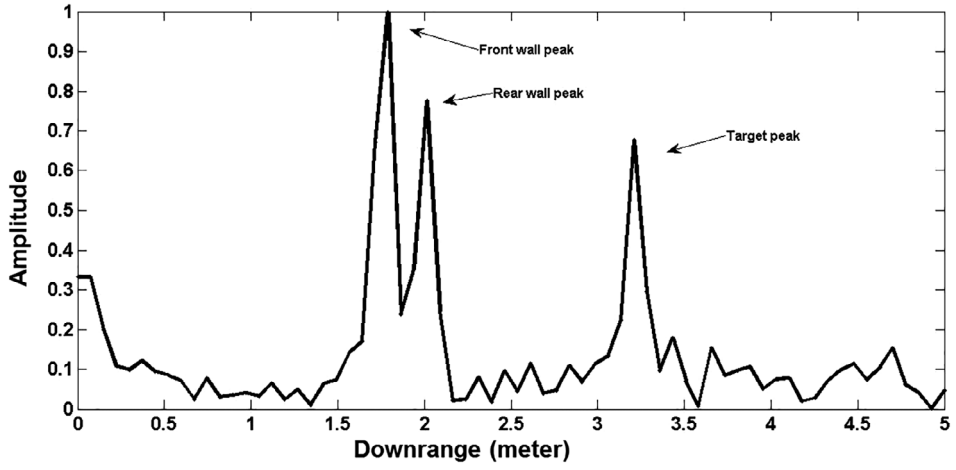

FIGURE 4 Corrected range profile plot

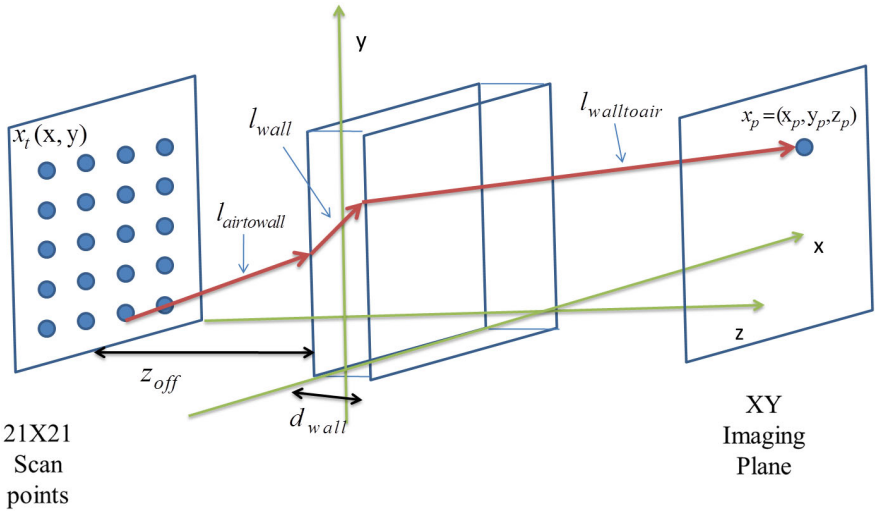

FIGURE 5 The geometry of through-the-wall imaging[5] [Color figure can be viewed at wileyonlinelibrary.com]

$$\begin{bmatrix} x_t' \\ y_t' \end{bmatrix} = \begin{bmatrix} cos\beta & sin\beta \\ -sin\beta & cos\beta \end{bmatrix} \begin{bmatrix} x_t \\ y_t \end{bmatrix} \tag{9}$$

$$\begin{bmatrix} x_{p_i}' \\ y_{p_i}' \end{bmatrix} = \begin{bmatrix} cos\beta & sin\beta \\ -sin\beta & cos\beta \end{bmatrix} \begin{bmatrix} x_{p_i} \\ y_{p_i} \end{bmatrix} \tag{10}$$

$$tan\beta = \frac{y_t - y_{p_i}}{x_t - x_{p_i}} \tag{11}$$

$$y_t' = y_q' \tag{12}$$

where x_t and y_t are antenna position and x_p and y_p are pixel position in xy plane.

Figures 6A-D show the raw 2-D TWRI image (crossrange vs height) of metallic rectangular (Target id-MRR1), metallic square (Target id-MSR1), wooden rectangle (Target id-WRR1), and wooden square (Target id-WSR1), target at 0° rotation, respectively. Detail description about target id is shown in Table A1. These 2D TWRI images provides useful information of the target extent in terms of length and height. Once optimal image processing methods are applied to these 2-D TWRI images (crossrange vs height) one can extract valuable information about target shape and size (ie, length and height). The raw 2D TWRI image will be further processed for the purpose of target recognition.

3.2.3 | Step 6. Image enhancement

The raw 2D C-scan image may contain unwanted pixels, other than desired target pixels, due to the background noise, multipath reflection, and other factors. Therefore, for enhancement of target pixels various image enhancement methods such as weiner filter, adaptive median filter, mean filter, and spatial maximum filter are considered. Performance of weiner filter, adaptive median filter, mean filter, and spatial maximum filter are examined[22] and are compared on the basis of PSNR as shown in Table 2.

$$MSE = \frac{1}{MXN}\sum_{i=1}^{N}\sum_{j=1}^{M}(F(i,j) - I(i,j))^2 \tag{13}$$

$$PSNR(\text{dB}) = 10\log\left(\frac{1}{MSE}\right) \tag{14}$$

where I represent a raw 2D image, F represents a filtered 2D image, M represents no of pixels in row and N represents no of pixels in columns. The image enhancement has been done using discrete convolution. In filtering operation, the pixels of an image is modified by moving the filter mask of size 3 × 3 from one pixel point to another pixel point of the image. After comparing the PSNR of all filtered images, it was found that the adaptive median filter provides good results in comparison with the other filtering operations. Figure 7A-D the enhanced 2D C-scan image of target id MRR1, WRR1, MSR1, and WSR1. The intensities of target pixels points in these images are significantly enhanced. The adaptive median filter also enhances the boundary of targets. This enhanced image is further used for detection and identification.

3.2.4 | Step 7. Statistic based thresholding technique

The statistic value of image plays a very important role to determine the boundary of targets. Therefore, the statistic based thresholding technique has been applied to determine the shape of target. The mean and SD of the image has been calculated and apply the threshold according to a given formula

$$T = mean(\mu) + n^{*}standarddeviation(\sigma) \tag{15}$$

The "n" is called a scaling parameter. The value of "n" has been determined by varying its value from 0 to 1 at 0.2 step size. We have found that n = 1.2 gives good results for metallic targets as wells as for wooden targets. The thresholded image of metallic rectangular has been shown in

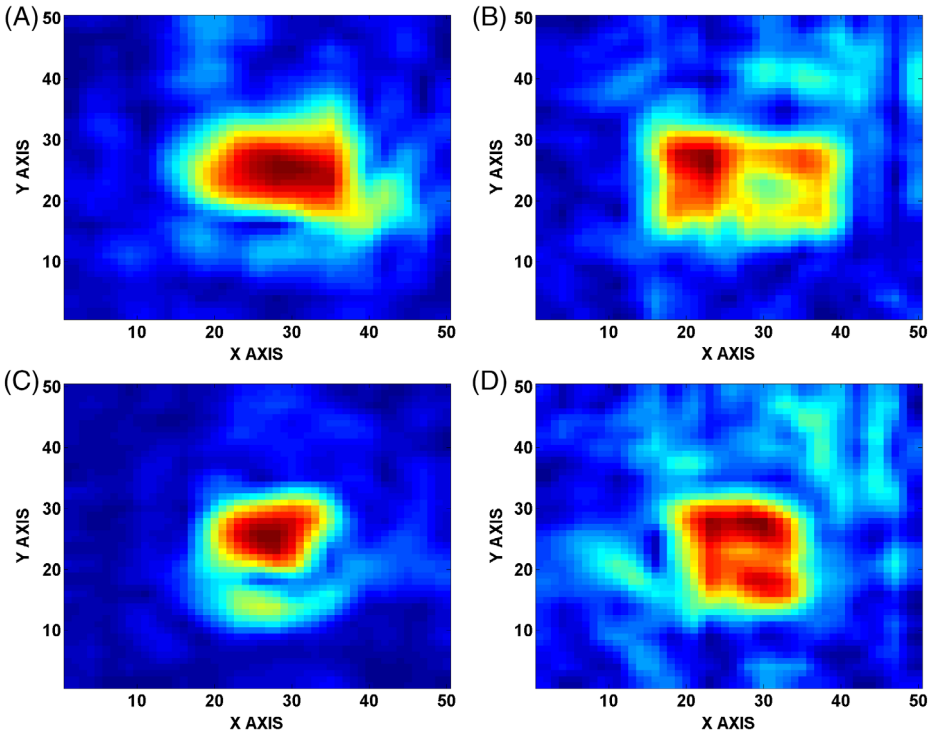

FIGURE 6 A, Raw 2D C-scan image obtained using delay and sum beamforming method on imaging plane along X and Y axis of target id MRR1. B, Raw 2D C-scan image obtained using delay and sum beamforming method on imaging plane along X and Y axis of target id WRR1. C, Raw 2D C-scan image obtained using delay and sum beamforming method on imaging plane along X and Y axis of target id MSR1. D, Raw 2D C-scan image obtained using delay and sum beamforming method on imaging plane along X and Y axis of target id WSR1 [Color figure can be viewed at wileyonlinelibrary.com]

TABLE 2 PSNR (dB) value of various spatial filtering techniques for target id MRR1, WRR1, MSR1, and WSR1

Filtering method	MRR1	WRR1	MSR1	WSR1
Spatial max	24.89	24.75	25.15	24.04
Mean	37.26	33.86	39.05	33.56
Weiner	40.68	37.28	41.9	36.56
Adaptive median	51	44.47	47.22	42.07

Figure 8A. The shape of targets is not as clear as it should be due to a few undesired pixel points have been observed in images after thresholding techniques. Now the ANN technique has been proposed to detect the actual shape of targets.

3.2.5 | Step 8. Scale invariant techniques for ANN

To increase the detection accuracy of the ANN model, numerous training data are required. The number of data can be increased with the help of multiple scanning of various targets behind the wall but it requires a long time. To save time, here, the data have been increased with the help of morphology technique. It is a tool that is used for extracting image components that are useful in the representation and description of region shapes, such as boundaries, skeletons, and convex hull. Dilation and Erosion are two operations that are fundamental to morphological filtering.[22] Dilation and Erosion are an operation that grows and compress or thickens and thin objects in a binary image, respectively. The "structuring element" controls the specific manner and extent or reduces of the image. Structuring elements are typically represented by a matrix of 1 and 0 second. Mathematically, dilation and erosion can be defined in terms of set operations as:

$$A \oplus B = \left\{ z | \left(\hat{B}\right)_z \cap A \neq \phi \right\} \tag{16}$$

where A is a thresholded image, B is the structuring element and φ is the empty set. The structuring element B = [1 1 1] increases and decreases the horizontal depth of image, the structuring element B = [1; 1; 1] increases and decreases the vertical depth of image and the structuring element B = [0 1 0; 1 1 1; 0 1 0] increases and decreases the vertical as well as horizontal depth of image by using dilation and erosion techniques, respectively. For example, the thresholded image of metal square target is (30 × 30 cm) is generated and after that apply dilation technique with structuring element B = [0 1 0; 1 1 1; 0 1 0], the obtained image corresponds to the metal square target whose size is (30 × 30 cm). The dilation technique extends the size of the image by 5 cm because one pixel size of image is (2.5 × 2.5 cm) and erosion technique reduces the size of the image by the same step. For making size invariant, the actual metal square target whose

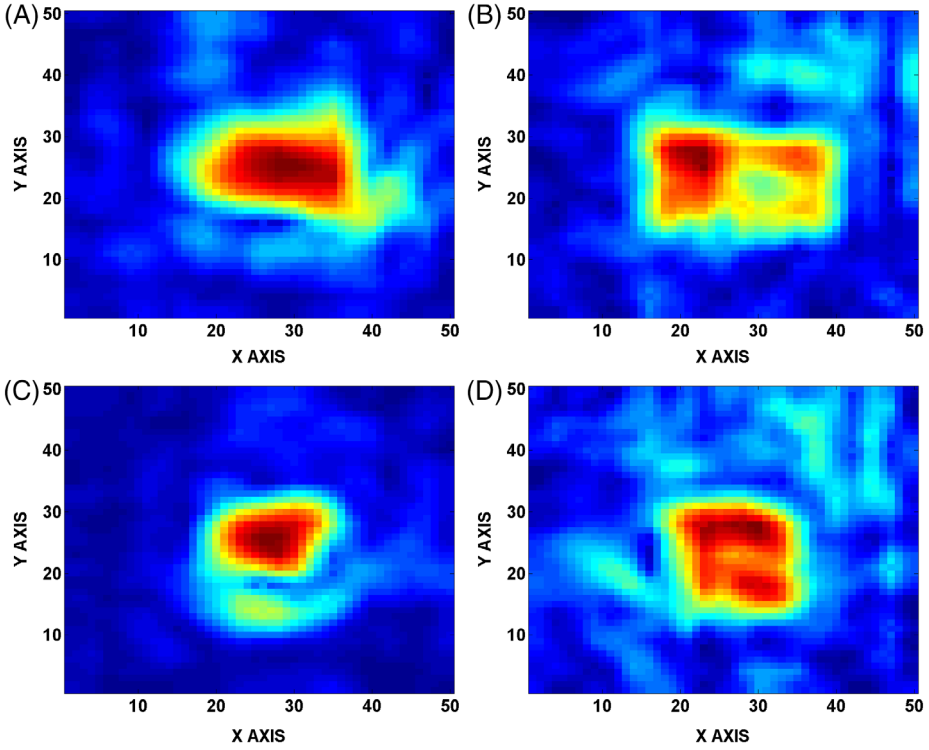

FIGURE 7 A, Adaptive median filtered image for target id MRR1. B, Adaptive median filtered image for target id WRR1. C, Adaptive median filtered image for target id MSR1. D, Adaptive median filtered image for target id WSR1 [Color figure can be viewed at wileyonlinelibrary.com]

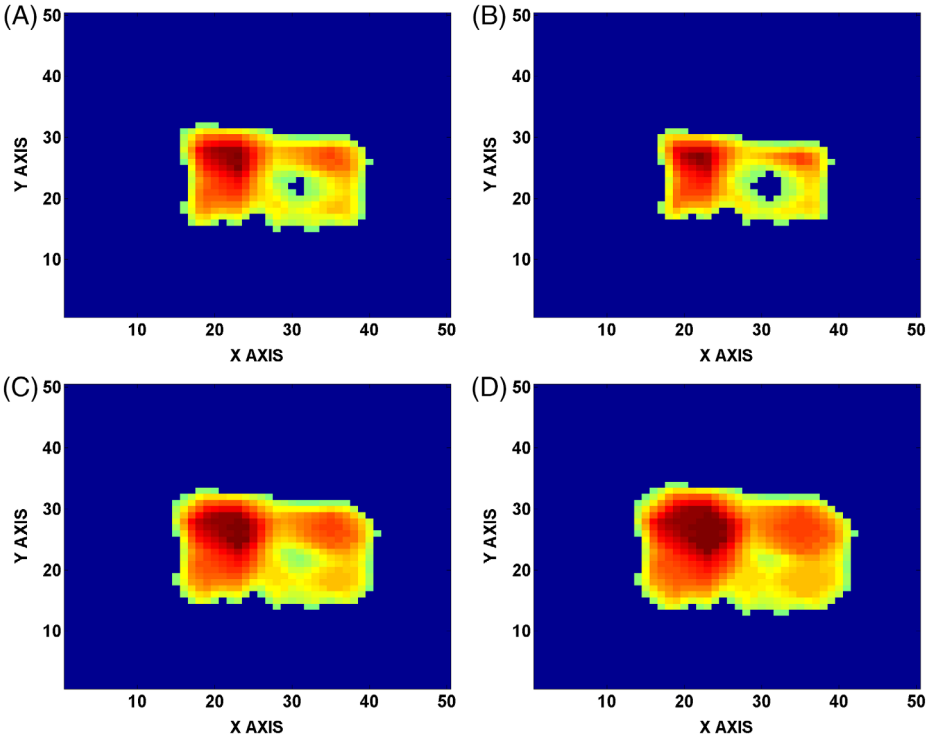

FIGURE 8 A, Statistics based thresholded 2D C-scan image of actual rectangular metal target of size 50 × 30 cm. B, Horizontally and vertically shrinked 2D C-scan image of rectangular metal target of size 25 × 45 cm obtained after applying morphological erosion technique on statics based thresholded 2D C-scan image of actual rectangular metal target of size 50 × 30 cm. C, Horizontally and vertically expanded 2D C-scan image of rectangular metal target of size 55 × 35 cm obtained after applying morphological dilation technique on statics based thresholded 2D C-scan image of actual rectangular metal target of size 50 × 30 cm. D, Horizontally and vertically expanded 2D C-scan image of rectangular metal target of size 60 × 40 cm obtained after applying morphological dilation technique on statics based thresholded 2D C-scan image of actual rectangular metal target of size 50 × 30 cm [Color figure can be viewed at wileyonlinelibrary.com]

TABLE 3 Results of image reconstructed for training data samples [Color table can be viewed at wileyonlinelibrary.com]

Actual target photograph	Thresholded 2D image	Reconstructed image using ANN	MSE
(1) Target Id—WTR2 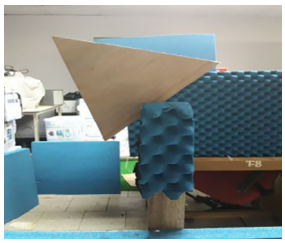	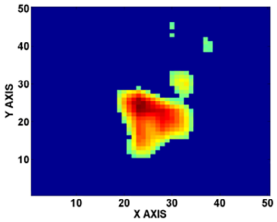	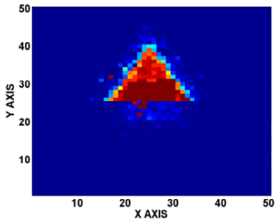	0.0065
(3)Target ID-MRR3 	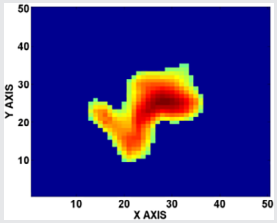	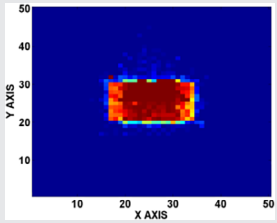	0.0168

size is (30 × 30 cm) has been scanned and the image has been generated for target size between (35 × 35 cm) and (40 × 40 cm) by using morphological techniques. The same techniques have been used for other shapes of targets. Few horizontally and vertically shrinked and expanded image of the metallic rectangular target have been shown in Figure 8 (B-D).

3.2.6 | Step 9. Target shape and size recognition using neural network

Our purpose is to recognize targets behind the wall from formed raw 2D TWRI image using a neural network. For this purpose, a multilayer feed forward neural network based for pattern recognition is considered with one hidden and output layer.[23] One of the major problems, which occur in recognizing the shape of the targets is with its orientation. It is difficult to identify the particular shape of the target with a slight orientation effect as shown in Table 3, which shows the raw image behind the wall at rotation angle 135. Thus, in order to make model rotation and size invariant many 2D C-scan images of the target in different shape, sizes, and orientation is required to train the ANN. For this purpose, we have collected C-scan data in different shape and orientation to generate its 2D C-scan image and used a morphological technique to generate 2D C-scan image of different sizes of targets. For example, 2D C-scan image of rectangular target of size (50 × 30) cm has been generated by real scanning of target and 2D C-scan image of rectangular target of size (55 × 35) cm and (60 × 40) cm have been generated by morphological techniques with structuring matrix [0 1 0; 1 1 1; 0 1 0], respectively. The details of the shape and size of the target considered with target id are given in Table A1.

The 18 samples of raw 2D TWRI image of size 50 × 50 are captured by TWRI system and the remaining 71 samples are generated by morphological technique. Thus, total 90 samples of data have been used to train the neural network as well as validation.

For training of the neural network, we have selected 81 (90%) samples out of the total of 90 data samples [samples having sr number 1 to 90 in Table A1]. The remaining nine samples were further used for testing on trained neural network. Among the 81 samples, we have randomly selected 70% of samples for training and the remaining 30% for validation, and testing point of view in a ratio of 15% and 15%, respectively. Hence, 81 samples have been selected for training the ANN and each sample represents 2D TWRI image of target in different shape, sizes, and orientations. The desired neural network configuration setup is shown in Figure 9 and consists of.

Input layer: Each of 2D C-scan image matrix (50X50) is transformed to column vector (50*50,1). In this way column vector of all 81 samples are stacked to form a 2D input matrix (50*50, 81). This input matrix is fed to an input layer of the neural network for training. This has enabled the proposed neural network to estimate size and shape of the target from 2D C-scan image for the considered target shape.

Hidden layer: The middle layer consist of 80 neurons. The numbers of neurons are chosen on the basis of trial and error in order to maintain the balance between ANN system complexity as well as minimizing the output error.

Output layer: In order to estimate the shape and size of the target, output-teaching matrix was assigned as a binary matrix according to the shape and size of the target considered. For example for the rectangle shape of size (50 × 30)

TABLE 4 Result of the image reconstructed for an independent test data samples [Color table can be viewed at wileyonlinelibrary.com]

Test target (Thresholded Image)	Output reconstructed image	MSE
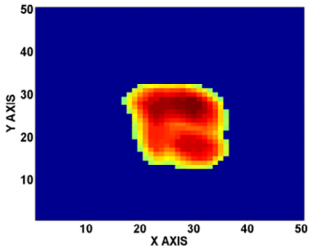 Target ID-WSV7	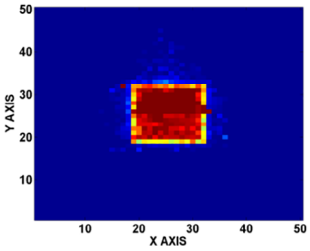	0.0135
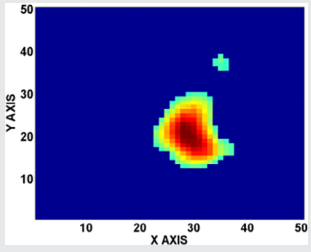 Target ID-WTR2	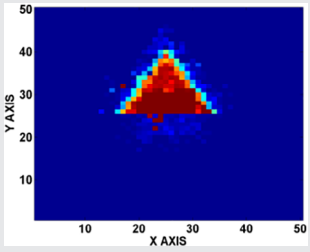	0.0071
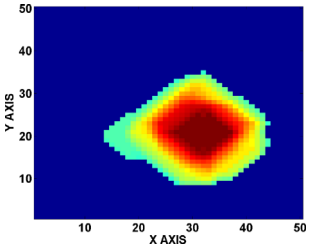 Target ID- WSV15	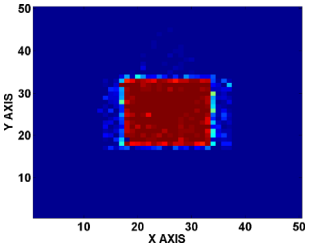	0.0208
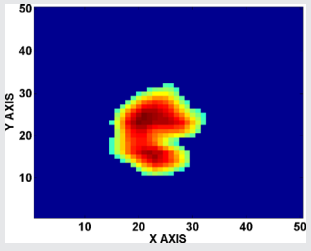 Target ID: MSR2	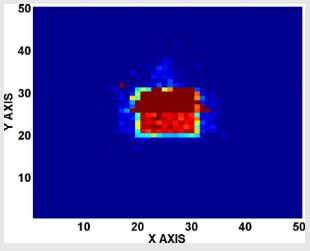	0.0122
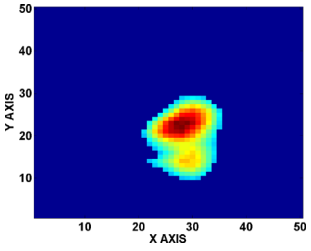 Target ID: MTR2	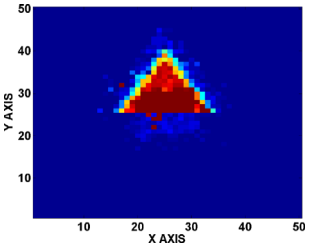	0.0072
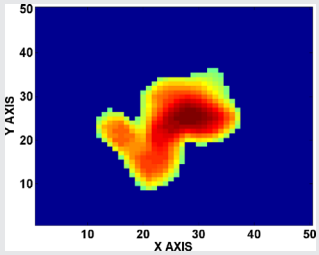 Target ID: MRV6	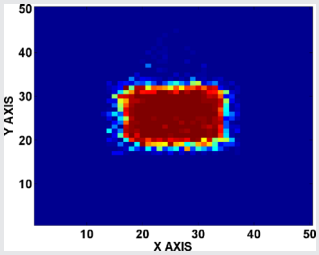	0.0215

TABLE 4 (Continued)

Test target (Thresholded Image)	Output reconstructed image	MSE
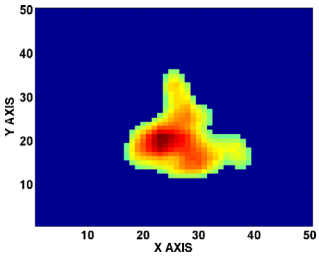 Target ID: WTR16	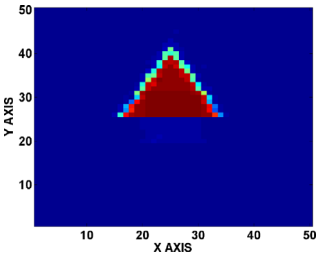	0.0487
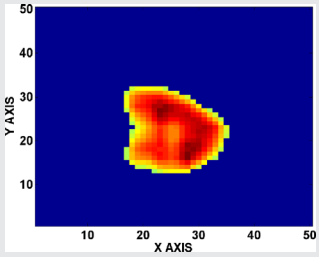 Target ID: WTR17	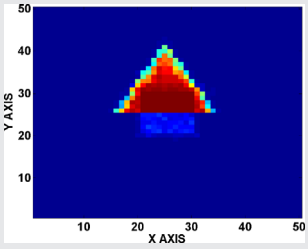	0.0494
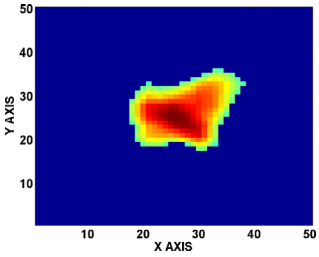 Target ID: WSR16	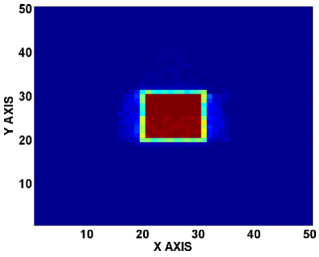	0.0053
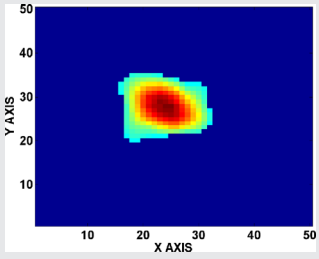 Target ID: WSR17	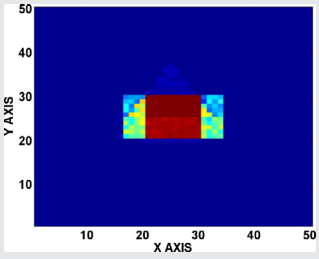	0.0155
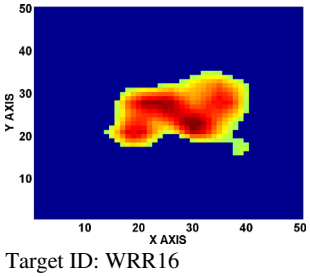 Target ID: WRR16	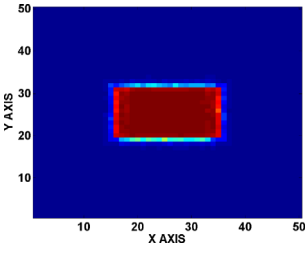	0.0021
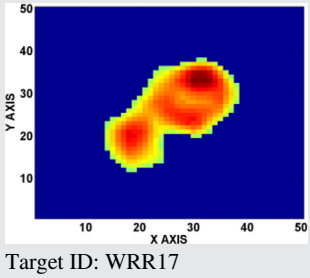 Target ID: WRR17	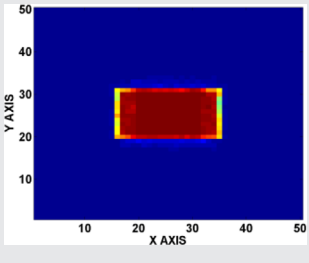	0.0019

TABLE 4 (Continued)

Test target (Thresholded Image)	Output reconstructed image	MSE
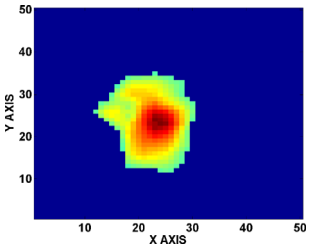 Target ID: MSR16	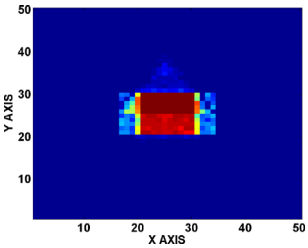	0.0111
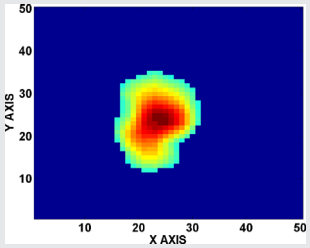 Target ID: MSR17	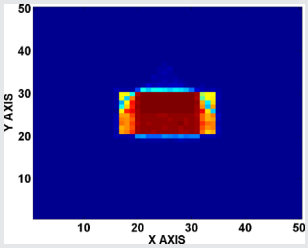	0.0166
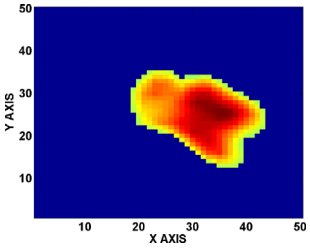 Target ID: MRR16	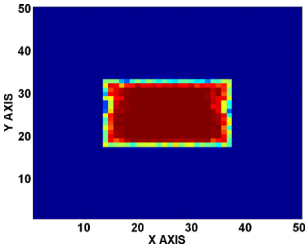	0.0311

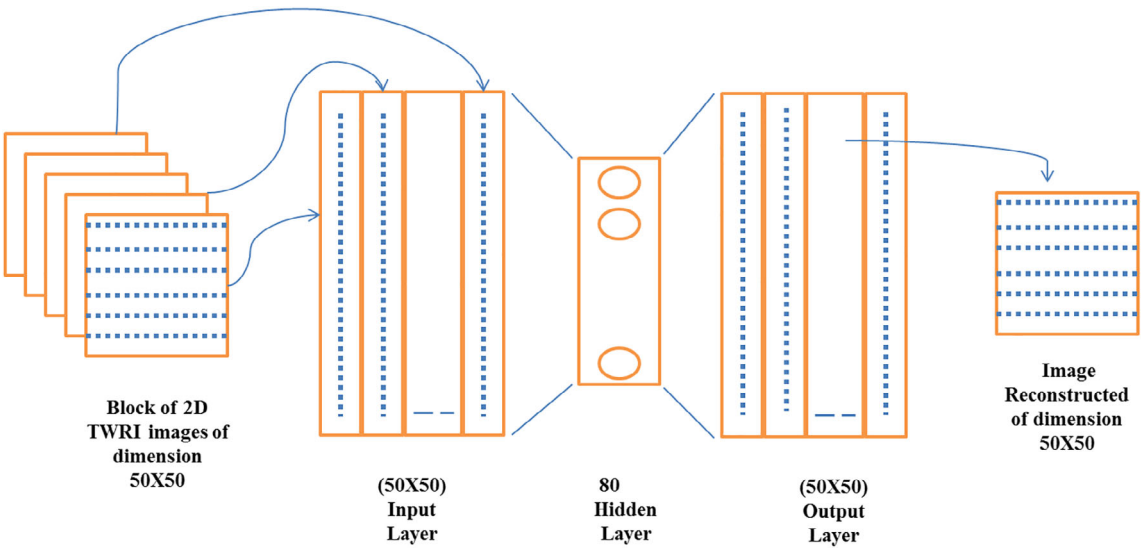

FIGURE 9 Neural network configuration model [Color figure can be viewed at wileyonlinelibrary.com]

is assigned a binary image to its corresponding rectangular target and rectangle shape of size (50×30) is assigned a binary image to corresponding rectangular target. Now rectangular shape target has been oriented to various angles and for each orientation binary matrix of the same size corresponding to rectangular target, size has been assigned because our aim is to estimate the shape. In this way, binary image assigned will be the same for any orientation of the same size.

A Sigmoid transfer function is chosen for the hidden and output layer so that the output of a neural network lies between 0 and 1 which is required for image reconstruction.

Mean squared error (MSE) criterion is used as a learning algorithm to train the neural network which is defined as

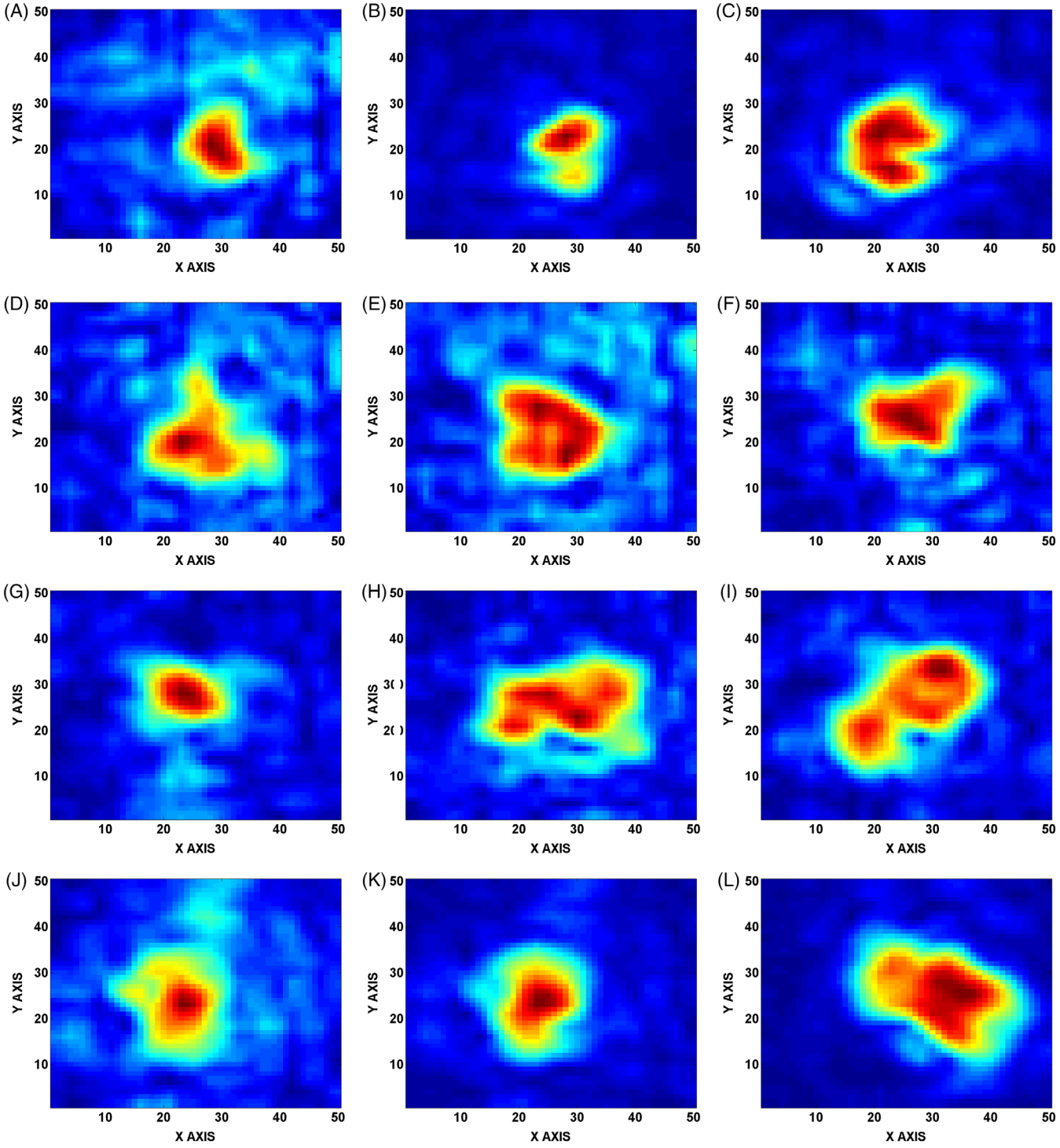

FIGURE 10 A, Raw image of targets id WTR2. B, Raw image of targets id MTR2. C, Raw image of targets id MSR2. D, Raw image of targets id WTR16. E, Raw image of targets id WTR17. F, Raw image of targets id WSR16. G, Raw image of targets id WSR17. H, Raw image of targets id WRR16. I, Raw image of targets id WRR17. J, Raw image of targets id MSR16. K, Raw image of targets id MSR17. L, Raw image of targets id MRR16 [Color figure can be viewed at wileyonlinelibrary.com]

$$mse = \frac{1}{N}\sum_{i=1}^{N} e_i^2 = \frac{1}{N}\sum_{i=1}^{N} (r_i - a_i)^2 \tag{17}$$

where "a" is the network outputs and "r" is the target outputs. In MSE criteria the neural network first produces its own output vector 'a' according to fed input vector and then compares the output vector.

4 | RESULTS

4.1 | Results of trained data samples

Table 3 shows the results of the image reconstructed using trained neural network for few data samples used for training that is, WTR3, and MRR3 (notations as per Table A1). Actual

photographs of the corresponding targets are also shown for reference. The Neural network has been trained using corresponding binary matrices, for example, target id WTR3, which is a wooden triangular shape having size 35 × 35 cm at 135° orientation, is assigned the same size and shape binary image and target id MRR3, which is a metallic rectangular shape having size 50 × 30 cm at 135° orientation, respectively, are assigned corresponding binary image. It can be inferred that trained neural network successfully reconstruct exact shape and size of the target for corresponding different shape and size of target at any orientation, with appreciably low MSE values, viz., 0.0065, 0.0168, respectively.

4.2 | Validation of developed ANN model for scale and rotation invariant

It is one of the most critical tasks to find the size and shape of targets behind the wall in case of different size and rotation. Different shape of targets behind the wall has been scanned and the corresponding size has been generated by morphological techniques. For example, the shape of target id MSR1, which is Metal Square having size 30 × 30 cm at 0° orientation, is really scanned and the image has been generated using delay-sum algorithm. The image of target id MSV4, which is a metal square having size 35 × 35 cm at 0° orientation, is generated by morphological techniques. It has saved the large scanning time. To generate the actual shape of targets, the ANN technique has been used. The thresholded delay-sum image is used to train the neural network with the help of corresponding binary image, for example, target id WTR1, which is wood triangular shape having size 35 × 35 cm at 0° orientation, is assigned the same size and shape binary image and target id WTV4 and WTV5, which is wood triangular shape having size 40 × 40 cm at 0° and 45° orientation, respectively, are assigned corresponding binary image. After training the neural network, the accuracy for scale and rotation invariant is verified by six independent data sets that are not used to train the network. These independent samples were fed to the trained neural network and a corresponding binary image is obtained as shown in Table 3. The MSE between the NN output image and the desired image is also shown.

Figures 10(A-L) show the raw image of the independent test samples of a wood triangular target of size 35 × 35 cm at 45° orientation, metal triangular target of size 35 × 35 cm at 45° orientation, metal square target of size 30 × 30 cm at 45° orientation, wood triangular target of size 50 × 50 cm at 0 orientation, wood triangular target of size 50 × 50 cm at 45 orientation, wood square target of size 35 × 35 cm at 0 orientation, wood square target of size 35 × 35 cm at 45 orientation, wood rectangular target of size 55 × 35 cm at 0 orientation, wood rectangular target of size 55 × 35 cm at 135 orientation, metal square target of size 35 × 35 cm at 0 orientation, metal square target of size 35 × 35 cm at 45 orientation, and metal rectangular target of size 55 × 35 cm at 135 orientation. As shown in Table 4, WTR2, MTR2 MSR2, WTR16, WTR17, WSR16, WSR17, WRR16, WRR17, MSR16, MSR17, and MRR16 target images are recognized as a output images having true size and shape, with MSE of 0.0078, 0.0023, 0.0063, 0.0487, 0.0494, 0.0053, 0.0155, 0.0021, 0.0019, 0.0111, 0.0166, and 0.0391, respectively which shows the capability of proposed rotation and scale invariant neural network for shape and size estimation of target for the considered regular target shapes. Thus the proposed neural network with these test samples shows good performance.

5 | CONCLUSION

In this article, a novel application of artificial neural network for recognition of shape and size of the target behind a wall using TWRI has been presented. For this purpose, an active microwave SFCW radar imaging system has been designed to capture the C-scan data of regular triangular, square, and wooden shape targets behind a wall. From these data, through the wall images are generated using a delay-sum beamforming algorithm. These images were segmented using statics based thresholding method and further used for training of artificial neural network for development of target recognition model. To develop a scale invariant ANN model, numerous thresholded TWRI for training is required. The number of TWRI can be increased with the help of multiple scanning of various targets behind the wall but it requires a long time. Therefore, to save the time, the TWRI has been increased with the help of morphology technique. The performance of various signal processing steps for target recognition has been validated by experimental results. The proposed neural network based signal processing technique ones trained with sample images have shown good performance with the test images and has recognized nearly actual shape and size of the target. This image reconstruction model using the artificial neural network can be further applied to rectify distorted microwave wave radar image caused due to variation in noise and orientation while acquisition.

ORCID

Akhilendra P. Singh https://orcid.org/0000-0002-2780-1073

REFERENCES

[1] Ahmad F, Amin MG, Kassam SA. Synthetic aperture beamformer for imaging through a dielectric wall. *IEEE Trans Aerosp Electron Syst*. 2005;41(1):271-283.

[2] Ahmad F, Amin MG, Kassam SA. Three dimensional wideband beamforming for imaging through a single wall. *IEEE Trans Aerosp Electron Syst*. 2005;41(1):271-283.

[3] Ahmad F, Amin MG. Noncoherent approach to through-the-wall radar localization. *IEEE Trans Aerosp Electron Syst*. 2006;42(4):1405-1419.

[4] Solimene R, Brancaccio A, Pierri R, Soldovieri F. TWI experimental results by a linear inverse scattering approach. *Prog Electromagn Res*. 2009;91:259-272.

[5] Wang G, Amin MG, Zhang Y. New approach for target locations in the presence of wall ambiguity. *IEEE Trans Aerospace Electron Syst*. 2006;42:301-315.

[6] Ahmad F, Amin MG, Mandapati G. Autofocusing of through-the-wall radar imagery under unknown wall characteristics. *IEEE Trans Image Process*. 2007;16:1785-1795.

[7] Li L, Zhang W, Li F. A novel auto-focusing approach for real-time through wall imaging under unknown wall characteristics. *IEEE Trans Geosci Remote Sens*. 2010;48:423-431.

[8] Jin T, Chen B, Zhou Z. Image-domain estimation of wall parameters for autofocusing of through-the-wall SAR imagery. *IEEE Trans Geosci Remote Sens*. 2013;51:1836-1843.

[9] Debes C, Amin MG, Zoubir AM. Target detection in single and multiple-view through-the-wall radar imaging. *IEEE Trans Geosci Remote Sens*. 2009;47(5):1349-1361.

[10] Verma PK, Gaikwad AN, Singh D, Nigam MJ. Analysis of clutter reduction techniques for through wall imaging in UWB range. *Prog Electromag Res B*. 2009;17:29-48.

[11] Debes C, Riedler J, Amin MG, and Zoubir AM, Iterative target detection approach for through-the-wall radar imaging. Paper presented at IEEE International Conference on Acoustics, Speech and Signal Processing, 2009, pp. 3061–3064.

[12] Gaikwad AN, Singh D, Nigam MJ. Application of clutter reduction of metallic and low dielectric target behind the brick wall by stepped frequency continuous wave radar in ultra-wideband range. *IET Radar Sonar Navig*. 2011;5:416-425.

[13] Tivive FH, Bouzerdoum A, Amin M. A subspace projection approach for wall clutter mitigation in through-the-wall radar imaging. *IEEE Trans Geosci Remote Sens*. 2015;53:2108-2121.

[14] Yoon YS, Amin MG. Spatial filtering for wall-clutter mitigation in through-the-wall radar imaging. *IEEE Trans Geosci Remote Sens*. 2009;47(9):3192-3208.

[15] Seng CH, Bouzerdoum A, Amin MG, Phung SL. Probabilistic fuzzy image fusion approach for radar through wall sensing. *IEEE Trans Image Proc*. 2013;22:4938-4951.

[16] Seng CH, Bouzerdoum A, Amin MG, Phung SL. Two stage fuzzy fusion with application to through the wall radar sensing. *IEEE Trans Geosci Remote Sens Lett*. 2013;10:687-691.

[17] Mobasseri BG and Rosenbaum Z, 3D classification of through-the-wall radar images using statistical object models. Paper presented at Proc IEEE Workshop Image Analy, Interpretation. 2008, pp. 149–152.

[18] Debes C, Hahn J, Zoubir AM, Amin MG. Target discrimination and classification in through-the-wall radar imaging. *IEEE Trans Signal Proc*. 2011;59(10):4664-4676.

[19] Hantscher S, Praher B, Reisenzahn A, CG Disk, Comparision of UWB target identification algorithm for through wall imaging application. Paper presented at Proceedings of the 3rd European Radar Conference, 2006.

[20] Gaikwad AN, Singh D, Nigam MJ. Recognition of target in through wall imaging in shape feature extraction. *IEEE IGARSS*. 2011.

[21] Muqaibal AH, Safaai-Jazi A. A new formulation for characterization of material based on measured insertion transfer function. *IEEE Trans Microwave Theory Tech*. 2003;51:1946-1951.

[22] Gonzalez RC, Woods RE. *Digital Image Processing*. 2nd ed. New Delhi: Pearson Education; 2007.

[23] Haykin S. *Neural Networks: A Comprehensive Foundation*. New York: Macmillan; 2005.

How to cite this article: Singh AP, Dwivedi S, Jain PK. A novel application of artificial neural network for recognition of target behind the wall. *Microw Opt Technol Lett*. 2020;62:152–167. https://doi.org/10.1002/mop.32020

APPENDIX

TABLE A1 List of target samples used for purpose of training and validation of neural network

S. No.	Shape	Target I/D	Size	Orientation	Material	Generated Image
	Triangle	WTR1	(Base × Height) = 35 × 35 cm	0	Wood	Real
	Triangle	WTR2	(Base × Height) = 35 × 35 cm	45	Wood	Real
	Triangle	WTR3	(Base × Height) = 35 × 35 cm	135	Wood	Real
	Triangle	WTV4	(Base × Height) = 30 × 30 cm	0	Wood	Virtual
	Triangle	WTV5	(Base × Height) = 30 × 30 cm	45	Wood	Virtual
	Triangle	WTV6	(Base × Height) = 30 × 30 cm	135	Wood	Virtual
	Triangle	WTV7	(Base × Height) = 40 × 40 cm	0	Wood	Virtual
	Triangle	WTV8	(Base × Height) = 40 × 40 cm	45	Wood	Virtual
	Triangle	WTV9	(Base × Height) = 40 × 40 cm	135	Wood	Virtual
	Triangle	WTV10	(Base × Height) = 45 × 45 cm	0	Wood	Virtual
	Triangle	WTV11	(Base × Height) = 45 × 45 cm	45	Wood	Virtual
	Triangle	WTV12	(Base × Height) = 45 × 45 cm	135	Wood	Virtual
	Triangle	WTV13	(Base × Height) = 50 × 50 cm	0	Wood	Virtual

TABLE A1 (Continued)

S. No.	Shape	Target I/D	Size	Orientation	Material	Generated Image
	Triangle	WTV14	(Base × Height) = 50 × 50 cm	45	Wood	Virtual
	Triangle	WTV15	(Base × Height) = 50 × 50 cm	135	Wood	Virtual
	Triangle	MTR1	(Base × Height) = 35 × 35 cm	0	Metal	Real
	Triangle	MTR2	(Base × Height) = 35 × 35 cm	45	Metal	Real
	Triangle	MTR3	(Base × Height) = 35 × 35 cm	135	Metal	Real
	Triangle	MTV4	(Base × Height) = 30 × 30 cm	0	Metal	Virtual
	Triangle	MTV5	(Base × Height) = 30 × 30 cm	45	Metal	Virtual
	Triangle	MTV6	(Base × Height) = 30 × 30 cm	135	Metal	Virtual
	Triangle	MTV7	(Base × Height) = 40 × 40 cm	0	Metal	Virtual
	Triangle	MTV8	(Base × Height) = 40 × 40 cm	45	Metal	Virtual
	Triangle	MTV9	(Base × Height) = 40 × 40 cm	135	Metal	Virtual
	Triangle	MTV10	(Base × Height) = 45 × 45 cm	0	Metal	Virtual
	Triangle	MTV11	(Base × Height) = 45 × 45 cm	45	Metal	Virtual
	Triangle	MTV12	(Base × Height) = 45 × 45 cm	135	Metal	Virtual
	Triangle	MTV13	(Base × Height) = 50 × 50 cm	0	Metal	Virtual
	Triangle	MTV14	(Base × Height) = 50 × 50 cm	45	Metal	Virtual
	Triangle	MTV15	(Base × Height) = 50 × 50 cm	135	Metal	Virtual
	Square	WSR1	(Length × width) = 30 × 30 cm	0	Wood	Real
	Square	WSR2	(Length × width) = 30 × 30 cm	45	Wood	Real
	Square	WSR3	(Length × width) = 30 × 30 cm	135	Wood	Real
	Square	WSV4	(Length × width) = 35 × 35 cm	0	Wood	Virtual
	Square	WSV5	(Length × width) = 35 × 35 cm	45	Wood	Virtual
	Square	WSV6	(Length × width) = 35 × 35 cm	135	Wood	Virtual
	Square	WSV7	(Length × width) = 40 × 40 cm	0	Wood	Virtual
	Square	WSV8	(Length × width) = 40 × 40 cm	45	Wood	Virtual
	Square	WSV9	(Length × width) = 40 × 40 cm	135	Wood	Virtual
	Square	WSV10	(Length × width) = 45 × 45 cm	0	Wood	Virtual
	Square	WSV11	(Length × width) = 45 × 45 cm	45	Wood	Virtual
	Square	WSV12	(Length × width) = 45 × 45 cm	135	Wood	Virtual
	Square	WSV13	(Length × width) = 50 × 50 cm	0	Wood	Virtual
	Square	WSV14	(Length × width) = 50 × 50 cm	45	Wood	Virtual
	Square	WSV15	(Length × width) = 50 × 50 cm	135	Wood	Virtual
	Square	MSR1	(Length × width) = 30 × 30 cm	0	Metal	Real
	Square	MSR2	(Length × width) = 30 × 30 cm	45	Metal	Real
	Square	MSR3	(Length × width) = 30 × 30 cm	135	Metal	Real
	Square	MSV4	(Length × width) = 35 × 35 cm	0	Metal	Virtual
	Square	MSV5	(Length × width) = 35 × 35 cm	45	Metal	Virtual
	Square	MSV6	(Length × width) = 35 × 35 cm	135	Metal	Virtual
	Square	MSV7	(Length × width) = 40 × 40 cm	0	Metal	Virtual
	Square	MSV8	(Length × width) = 40 × 40 cm	45	Metal	Virtual
	Square	MSV9	(Length × width) = 40 × 40 cm	135	Metal	Virtual
	Square	MSV10	(Length × width) = 45 × 45 cm	0	Metal	Virtual
	Square	MSV11	(Length × width) = 45 × 45 cm	45	Metal	Virtual

TABLE A1 (Continued)

S. No.	Shape	Target I/D	Size	Orientation	Material	Generated Image
	Square	MSV12	(Length × width) = 45 × 45 cm	135	Metal	Virtual
	Square	MSV13	(Length × width) = 50 × 50 cm	0	Metal	Virtual
	Square	MSV14	(Length × width) = 50 × 50 cm	45	Metal	Virtual
	Square	MSV15	(Length × width) = 50 × 50 cm	135	Metal	Virtual
	Rectangle	WRR1	(Length × width) = 50 × 30 cm	0	Wood	Real
	Rectangle	WRR2	(Length × width) = 50 × 30 cm	45	Wood	Real
	Rectangle	WRR3	(Length × width) = 50 × 30 cm	135	Wood	Real
	Rectangle	WRV4	(Length × width) = 55 × 35 cm	0	Wood	Virtual
	Rectangle	WRV5	(Length × width) = 55 × 35 cm	45	Wood	Virtual
	Rectangle	WRV6	(Length × width) = 55 × 35 cm	135	Wood	Virtual
	Rectangle	WRV7	(Length × width) = 45 × 25 cm	0	Wood	Virtual
	Rectangle	WRV8	(Length × width) = 45 × 25 cm	45	Wood	Virtual
	Rectangle	WRV9	(Length × width) = 45 × 25 cm	135	Wood	Virtual
	Rectangle	WRV10	(Length × width) = 60 × 40 cm	0	Wood	Virtual
	Rectangle	WRV11	(Length × width) = 60 × 40 cm	45	Wood	Virtual
	Rectangle	WRV12	(Length × width) = 60 × 40 cm	135	Wood	Virtual
	Rectangle	WRV13	(Length × width) = 65 × 45 cm	0	Wood	Virtual
	Rectangle	WRV14	(Length × width) = 65 × 45 cm	45	Wood	Virtual
	Rectangle	WRV15	(Length × width) = 65 × 45 cm	135	Wood	Virtual
	Rectangle	MRR1	(Length × width) = 50 × 30 cm	0	Metal	Real
	Rectangle	MRR2	(Length × width) = 50 × 30 cm	45	Metal	Real
	Rectangle	MRR3	(Length × width) = 50 × 30 cm	135	Metal	Real
	Rectangle	MRV4	(Length × width) = 55 × 35 cm	0	Metal	Virtual
	Rectangle	MRV5	(Length × width) = 55 × 35 cm	45	Metal	Virtual
	Rectangle	MRV6	(Length × width) = 55 × 35 cm	135	Metal	Virtual
	Rectangle	MRV7	(Length × width) = 45 × 25 cm	0	Metal	Virtual
	Rectangle	MRV8	(Length × width) = 45 × 25 cm	45	Metal	Virtual
	Rectangle	MRV9	(Length × width) = 45 × 25 cm	135	Metal	Virtual
	Rectangle	MRV10	(Length × width) = 60 × 40 cm	0	Metal	Virtual
	Rectangle	MRV11	(Length × width) = 60 × 40 cm	45	Metal	Virtual
	Rectangle	MRV12	(Length × width) = 60 × 40 cm	135	Metal	Virtual
	Rectangle	MRV13	(Length × width) = 65 × 45 cm	0	Metal	Virtual
	Rectangle	MRV14	(Length × width) = 65 × 45 cm	45	Metal	Virtual
	Rectangle	MRV15	(Length × width) = 65 × 45 cm	135	Metal	Virtual
	Triangle	WTR16	(Base × Height) = 50 × 50 cm	0	Wood	Real
	Triangle	WTR17	(Base × Height) = 50 × 50 cm	45	Wood	Real
	Square	WSR16	(Length × width) = 35 × 35 cm	0	Wood	Real
	Square	WSR17	(Length × width) = 35 × 35cm	45	Wood	Real
	Square	MSR16	(Length × width) = 35 × 35 cm	0	Metal	Real
	Square	MSR17	(Length × width) = 35 × 35 cm	45	Metal	Real
	Rectangle	WRR16	(Length × width) = 55 × 35 cm	0	Wood	Real
	Rectangle	WRR17	(Length × width) = 55 × 35 cm	135	Wood	Real
	Rectangle	MRR16	(Length × width) = 55 × 35 cm	45	Metal	Real